[Re] Computational Modelling of Glucose Uptake by SGLT1 and Apical GLUT2 in the Enterocyte

Karim Raqbi, Maxime Folschette, Cristian Versari, Olivier Briand, Cédric Lhoussaine

RESCIENCE C

Replication / Bioinformatics

[Re] Computational Modelling of Glucose Uptake by SGLT1 and Apical GLUT2 in the Enterocyte

Karim Raqbi[1,2], Maxime Folschette[1], Cristian Versari[1], Olivier Briand[2], and Cedric Lhoussaine[1]
[1]Univ. Lille, CNRS, Centrale Lille, UMR 9189 CRIStAL, F-59000 Lille, France – [2]Univ. Lille, Inserm, CHU Lille, Institut Pasteur de Lille, U1011- EGID, F-59000 Lille, France

Edited by
Konrad Hinsen

Reviewed by
Gleb Pogudin
Konrad Hinsen

Received
21 October 2025

Published
10 June 2026

DOI
10.5281/zenodo.20613595

1 Abstract

This article is the reproduction of the computational model of glucose absorption by the enterocyte by Afshar et al. in 2021 [1] and more precisely, the reproduction made by the authors themselves in 2023 [2]. The enterocyte is the main component of the intestinal barrier, that is the cell type transporting glucose from digested food in the intestine to the blood. To this day, the model from Afshar et al. is the most complete description of enterocyte absorption, defined in terms of ordinary differential equations for the glucose, the ionic species and other physical properties of the cell.
This paper presents a complete reengineering and rewriting of this model in a different language, from CellML to Julia, with added comments and bibliography. We reproduce each figure of the original paper and comment on their meaning. Our reproduction is freely available with the following link [3] and can be easily modified for reuse and modification of the model and its parameters.
It should also be noted that Afshar et al. also inversed the sign of the paracellular flux of glucose but since the relative value of this flux is negligible compared to the fluxes through the cell, the difference is insignificant.

2 Introduction

This article reproduces the model of Afshar et al. in 2021 [1], more precisely, the reproduction made by the authors themselves in 2023 [2], which is defined in terms of ordinary differential equations and implemented in CellML.
This introduction first presents some biological background in Subsection 2.1 and of existing computational models of the enterocyte in Subsection 2.2. Then, Section 3 presents the tools and methods used to reproduce this model in Julia, and Section 4 compares the results with the original article [2]. Finally, Section 5 concludes and gives some perspectives.

2.1 Background

Enterocytes are the major cellular subtype forming the intestinal epithelium. These polarized epithelial cells (with specialized apical and basolateral membranes) cover the

Correspondence should be addressed to Cedric Lhoussaine (Cedric.Lhoussaine@univ-lille.fr)
The authors have declared that no competing interests exist.
Code is available at https://gitlab.univ-lille.fr/cedric.lhoussaine/glucoseuptake_sglt1_glut2. – SWH swh:1:dir:f9aa17e5cfe4de39b8f5fa7d61f10979bd82a8ef.
Open peer review is available at https://github.com/ReScience/submissions/issues/96.

inner face of the intestine, forming an active barrier which allow the transport of nutrients, including glucose, from the intestinal lumen to the intersticial space. The nutrients then reach the systemic bloodstream through the capillaries.
Biologists have identified three different means of glucose transport at the cellular level of enterocytes (see Figure Enterocyte). To this date, their relative contribution to intestinal absorption is up to debate. The first transport is mediated by SGLT1, a sodium/glucose cotransporter located in the apical membrane of the enterocyte (the membrane facing the intestinal lumen). SGLT1 cotransports glucose along with two sodium ions (high affinity, low capacity) [4]. Subsequently, the accumulated intracellular glucose is released in the basolateral compartment (the space at the enterocyte base communicating with capillaries and bloodstream) via the GLUT2 transporter located on the basolateral membrane.
The second transport pathway involves the translocation of GLUT2 to the apical membrane as reported to occur a response to high glucose luminal content [5]. In that case, apical GLUT2 generates a passive flux of glucose from the intestinal lumen into the cell [5, 6], while it is still present on the basolateral side to release glucose from the cell to the blood.
The last transport mechanism is the paracellular pathway where a flux of glucose is assumed between the cells. The impermeable tight junctions between the enterocytes would be loosened to allow glucose to flow through [7].
The model of Afshar et al. includes all three modes of glucose uptake by the enterocytes, as all these pathways may coexist.

2.2 State of the Art

To the best of our knowledge, the first model of glucose absorption by enterocytes was published by Thorsen et al. in 2014 [8]. This model, implemented in Matlab and Simulink, describes the ionic fluxes in the enterocytes but lacks the possibility of GLUT2 translocation in the apical membrane and does not include the paracellular pathway. Naftalin then published his own model [9], implemented with Berkeley Madonna (a modelling software package), with a focus on glucose and water absorption by enterocytes along the intestine. Rather than glucose absorption, this work addresses the possible controle of volume homeostasis by apical GLUT2. That model was used by Afshar et al. [1] to compare their results on the volume homeostasis with that model.
Afshar et al. published their first model in 2019 [10], followed by a second one in 2021 [1]. These models are written in CellML [11], an open standard based on XML, which can be handled by OpenCOR [12], a modeling environment that allows for a human friendly edition and simulation of CellML models.
Afshar et al. reproduced their own results and figures published in [10] and [1] in separate papers ([13] and [2] respectively).
Their first paper in 2019 [10] is an extension of Thorsen et al. [8] with the decomposition of the sodium/chloride co-transport, the addition of several ionic transporters and a focus on the respective roles of SGLT1 and GLUT2 in glucose transport. This article was followed by a reproduction paper in 2020 [13]. The second paper in 2021 [1] is a second version of the model in which the cellular volume is included as a variable to simulate water transport. It was followed by a second reproduction paper in 2023 [2]. The Python files necessary to obtain the precise parameter values chosen for each figure were only included in the reproduction papers from 2020 and 2023, which allowed for the direct rerunning of some of the figures with OpenCOR.
Moreover, all papers exhibit differences in both their governing equations and parameter values. These discrepancies are observed even between a paper and its direct reproduction, sometimes for identical biological components.

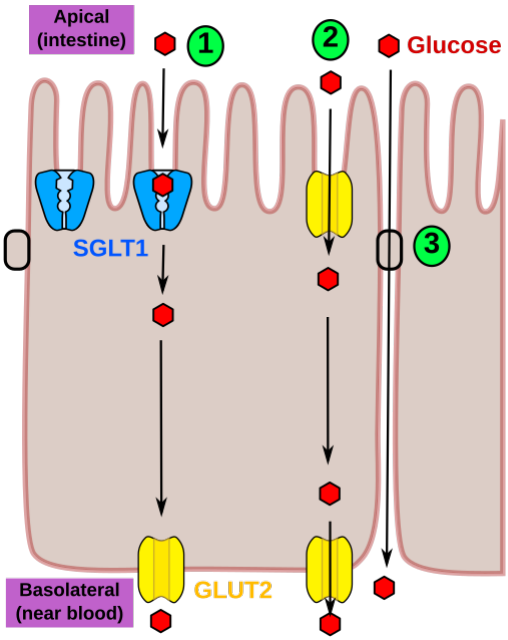

Figure Enterocyte. Representation of the three pathways for glucose transport. **1:** The glucose (red hexagones) enter the cell through the SGLT1 transporter (in blue) from the apical side (facing the intestine), then GLUT2 (yellow) releases it in the basolateral side (facing the capillaries and the blood flow). **2 :** When glucose concentration in the intestine is high, GLUT2 can also be located to the apical membrane, increasing glucose entry into the cell, still followed by a release by basolateral GLUT2 to the basolateral compartment. **3 :** The third pathway of glucose transport described is paracellular. The impermeable barrier (tight junctions) between cell is dynamically loosened to allow the glucose to flow in between the cells.

3 Methods

As it is the only paper for which all the Python codes and actual parameter values are available to reproduce each figure, we focused on the very last reproduction paper of 2023 [2].
The model that comes with these articles consists of 12 ordinary differential equations (ODEs), 250 algebraic equations and 261 parameters.

3.1 Model Re-implementation

We reimplemented this model in Julia, an open source, modern general-purpose programming language. Julia is particularly well suited for numerical and scientific computing with a rich ecosystem of packages, especially packages specialized in modeling, simulation and analysis of ODE systems. As a general-purpose language, it allows a greater expressiveness compared to a specialized environment such as OpenCOR, and makes modification, extension and analysis easier.+ We were able to reproduce all the figures of [2].
The Julia package CellMLToolkit (v2.14.0) proved valuable to import the CellML model in Julia for debugging purposes. However, we could not use it because the resulting encapsulated data structure prohibited modification and extension, so it could not be used to reproduce the figures.
The reproduction of the model of [2] happened to be challenging partly due to the lack of a README file and comments in the code. The files contained redundancies, parameters with identical names (for different compartments of the model), and unused

equations and parameters. Some equations appeared to be derived from earlier studies or to represent artifacts of planned but unimplemented model features. In addition, several parameters and equations were strictly identical for apical and basolateral GLUT2, reflecting the fact that they correspond to the same biological molecule with different membrane localizations. Therefore, we cleaned the model by removing superfluous equations and parameters, reducing the number of algebraic equations from 250 to 126, and the number of parameters from 261 to 119. Then, we renamed some parameters and variables to get a unified and clear nomenclature. We rewrote the whole set of differential and algebraic equations in Julia using the ModelingToolkit package (ModelingToolkit v9.80.6) [14], a symbolic-numeric computation package dedicated to scientific computing.
Finally, we sorted the equations and parameters in the code by biological function and added a documentation to the best of our knowledge.

3.2 Model Debugging

The process of rewriting the model and addressing the discrepancies between the original Afshar et al. model [1] and the reproduction paper [2] introduced several errors into our Ordinary Differential Equation (ODE) system. We successfully tackled these errors by comparing our results against outputs from OpenCOR and the CellMLToolkit import. This rigorous debugging process not only validated our equations but also allowed us to precisely identify undocumented parameter differences across the figures in the source paper (see Section 4).

3.3 Outcome

We can now assert to have a faithful reproduction of the model of Afshar et al. in 2023 [2], since the relative difference between their model and our reproduction stays below numerical precision, which allowed us to reproduce all their figures with the exception of the error bars in Figure 2 (see 4.0.2).
The code is freely available, here [3] under the CeCILL-C Free Software License Agreement. The equations and parameters were documented to the best of our knowledge with their line number in the original CellML source code, in the corresponding scientific papers, as well as their meaning in biology. To do so, we created a Julia dictionnary with for each equation, a dictionary was created gathering the corresponding line in the code of Afshar et al., the transporter it is linked to, and the biological meaning of the associated variable when known.
It should also be noted that Afshar et al. also inversed the sign of the paracellular flux of glucose but since the relative value of this flux is negligible compared to the fluxes through the cell, the difference is insignificant.

4 Results and Discussion

The figures are reproduced in the same order and numbered identically as in [2]. We observed that parameters were altered across figures, as detailed in Table 1, despite the lack of mention in the source paper [2]. Also, the equations written in [1] do not always match with their implementation, and some variations, both in the equations and in the parameter values, were identified from the paper in 2021 and its reproduction by the authors in 2023.
Table 1 documents the parameter values, which were found to vary between figures, a detail that is not mentioned in [1] and [2]. Specifically, the quantities of the transporters (apical GLUT2 (`n_GLUT_ap`), basolateral GLUT2 (`n_GLUT_bl`), and SGLT1 (`n_SGLT1`)) can change by as much as 10-fold across the figures.

Variations in `Glc_in` (the glucose influx into the basolateral compartment originating from the upstream blood flow) also significantly impact the steady state. Furthermore, we report that the values of `k_12_0` and `k_61_0` were modified for some figures. Since these parameters quantify the physical properties (reaction speed) of the SGLT1 transporters, they are biologically expected to remain constant.

Parameter	Figure 1	Figure 2	Figure 3	Figure 4	Figure 5	Figure 6	Figure 7
`cell_Na_c`	0.045	0.09	0.15	0.15	0.15	0.15	0.15
`cell_K_c`	0.105	6×10^{-3}	5.4×10^{-3}	5.4×10^{-3}	5.4×10^{-3}	5.4×10^{-3}	5.4×10^{-3}
`cell_Cl_c`	0.057	0.09	0.15	0.15	0.15	0.15	0.15
`L_ap`	6×10^{-5}	6×10^{-5}	6×10^{-5}	6×10^{-5}	6×10^{-6}	5×10^{-5}	6×10^{-5}
`L_bl`	6×10^{-5}	6×10^{-5}	6×10^{-5}	6×10^{-5}	6×10^{-6}	5×10^{-5}	6×10^{-5}
`V_bl`	1×10^{-16}	1×10^{-16}	1×10^{-16}	1×10^{-16}	1×10^{-16}	1×10^{-17}	1×10^{-17}
`Glc_in`	5×10^{-3}	5×10^{-3}	0.004	0.004	5×10^{-3}	5×10^{-3}	0.004
`n_GLUT_ap`	2×10^{8}	2×10^{9}	2×10^{8}	variable	variable	variable	1e8 / variable
`n_GLUT_bl`	2×10^{8}	2×10^{9}	2×10^{8}	variable	variable	variable	3e7 / variable
`n_SGLT1`	3×10^{7}	1×10^{8}	3×10^{7}	variable	4×10^{7}	variable	6×10^{7}
`Q_in`	1×10^{-17}	2×10^{-17}	2×10^{-17}	9×10^{-18}	9×10^{-18}	1×10^{-17}	9×10^{-18}
`k_12_0`	12000	14000	14000	12000	12000	14000	12000
`k_61_0`	15	25	25	15	15	25	15
`G_ENaC`	0.5	1.6	1.6	1.6	1.6	1.6	1.6
`apical_Glc_c`	0.05	variable	0.05	0.05	0.05	0.05	0.05

Table 1. Parameters and initial concentrations were modified from their default values and varied between figures without explicit documentation. Any parameter or initial concentration is designated as "variable" if it was investigated across multiple runs within a single figure.

Dynamic behavior of the model in response to an injection of apical glucose — Figure 1 shows the temporal variation of several key model variables and their response to an apical glucose input at $t = 5000s$. The original figure is cropped to start from $t = 2000s$ which obfuscates the first variations of these variables. The curves in the first 2000 seconds show that the model is not initially at steady-state which is reached at about 3000 seconds.

Comparison of absorption rates against experimental values — In Figure 2, Afshar et al. [1] compare the result of their model, more specifically of the absorption of glucose, sodium and water by the intestine, with experimental data from Collin et al. [15].
In this figure, the panel labeled "Glucose Absorption" represents a specific process: the absorption from the cell to the basolateral compartment via GLUT2 (the yellow transporter shown at the cell's base in Figure Enterocyte). It is not the total basolateral absorption (as commonly implied), as it deliberately excludes the paracellular absorption pathway, even though that pathway is included elsewhere in the model.
Moreover, the "Sodium Absorption Rate" represents only the sodium absorbed by the cell, not the total absorption into the basolateral compartment. Consequently, this rate does not reflect the measurements from Collins et al. However, obtaining precise experimental data for cellular sodium concentration and absorption would be extremely challenging, and no precise data is available to the best of our knowledge.
The values shown represent the mean and standard deviation obtained from four seperate runs where the parameter `Q_in` was varied $[6 \times 10^{-18}, 1 \times 10^{-17}, 3 \times 10^{-17}, 1 \times 10^{-15}]$. We were unable to determine the rationale for the choice of these specific values. As `Q_in` is associated with capillary blood flow, its variation affects the basolateral input (glucose, potassium, sodium, and chloride) from the blood, as well as the subsequent flush-out of these molecules.
Although we successfully reproduced the mean values, we could not replicate the error bars shown by Afshar et al. This is because the error bars were hard-coded in the authors' Python script and not generated via calculation.

In addition, we failed to reproduce the experimental bars in the figure. Collins et al. [15] tried to determine if electrical stimulation of a segment of dog intestine could influence the absorption of glucose sodium and water. We suppose that the data comes from Figure 2 of [15] for the volume, Figure 3 for glucose and Figure 4 for sodium, so we measured from the figure directly the heights of the bars for the four different dogs to get the experimental value obtained, from the period I before pacing. We then applied the conversion ratio to reach the unit chosen by Afshar et al., by choosing an estimated number of cells of 1.3×10^9 (as written in [1]). Our recalculation of the experimental values shows major differences (about 2-fold for glucose, more than ten-fold for water absorption rate). We reported the recalculation of this experimental measurement to be compared to Afshar et al. in Figure 2-bis.

Role of apical GLUT2 for different concentrations of apical glucose — In Figure 3, Afshar et al. study the influence of apical glucose and the apical GLUT2 transporter on different variables. Note that, for some unknown reason, the first value at 0 mM apical glucose of the blue curve (with GLUT2) is obtained with a quantity `n_GLUT_ap` (quantity of apical GLUT2) halved (0.5×10^8) compared to the other points (1×10^8). We tested without this modification and the results are similar.
Remark that the model of Afshar et al. predicts a cell shrinking when exposed to high concentrations of apical glucose. To our knowledge, this was not reported by any *in vivo* or *in vitro* experiment and might be worth investigating.

Study of different densities of glucose transporters — Figure 4 in this paper studies the influence of different quantities of glucose transporters, namely apical GLUT2, basolateral GLUT2 and SGLT1.

Role of the capillary flow and the mode of GLUT2 relocation and impact on glucose transport — Figure 5 is a sensitivity analysis, where parameters are varied in each row to study their effect on the final steady-state values of the model's main variables.
The first row of this figure studies the influence of `Q_in` (plotted on the x-axis), which represents the capillary blood flow. An increased `Q_in` enhances the exchange rate: systemic blood species (such as glucose and sodium) are faster supplied to the basolateral compartment, and basolateral species are more rapidly flushed out into the general circulation. Consequently, the basolateral concentration of these species converges more closely toward their systemic plasma values.
Rows two and three show the influence of two modes of GLUT2 appearance to the apical side (see pathway **2** in Figure Enterocyte). The second row is the scenario where GLUT2 is translocated from the basolateral membrane to the apical one, so the transporters are taken from one pool to the other (the horizontal axis is the quantity of apical and basolateral GLUT2). In the third row, GLUT2 does not come from the basolateral side and goes directly to the apical membrane (horizontal axis is the variation of apical GLUT2 from half its standard value, to double its value). Biologically, it would mean that a pool of GLUT2 could be stored in vesicles and added to the apical membrane. To the best of our knowledge, the available biological evidence does not definitively favor either hypothesis, leaving both as credible possibilities.
The fourth row shows variation of `Glc_in`, the influx from blood to the basolateral side which may reflect a patient with hyperglycemia (higher basal glucose levels). As in the model both SGLT1 and GLUT2 are bidirectional and have their fluxes dependant on the concentrations in both compartment, increase in `Glc_in` explains the decrease in the fluxes of the transporters in the model.
The first `Q_in` is set to 4.5×10^{-18} instead of 5×10^{-18} (for `Q_in` is set to 10^{-17} by default). This is probably a typo by the authors, and the correction of that parameter does not change much the results of the figure published by Afshar et al. [1].

We noted a typo in the 2021 paper [1], both in the caption and in the text of the corresponding figure: (**F-J**) is described as the response to variations in inlet blood glucose while it is actually the fourth row (**P-T**).

	Cond 1	Cond 2	Cond 3	Cond 4	Cond 5
$n_{GLUT_{ap}}$	0	0.5×10^8	1×10^8	5×10^7	1×10^5
$n_{GLUT_{bl}}$	2×10^8	1.5×10^8	1×10^8	1.5×10^8	2×10^8
n_{SGLT1}	4×10^7	6×10^7	4×10^7	8×10^7	8×10^7

Table 2. Values of the different quantities of glucose transporters for each bar in the histograms of Figure 6.

Study of different combinations of SGLT1 and GLUT2 quantities — Figure 6 shows the final value (steady state) of glucose in the basolateral compartment, glucose in the cell, and flux of glucose through the GLUT2 in the basolateral membrane. The bars correspond to different sets of parameters for glucose transporters quantity as reported in Table 2. Condition 1 is without apical GLUT2 and $2e8$ basolateral GLUT2. Condition 3 is similar to condition 1, but with a translocation of GLUT2 from the basolateral to the apical side with half the initial quantity of basolateral GLUT2 going to the apical membrane.

Comparison of the cell volume with the simulations from Naftalin — In Figure 7, Afshar et al. [1] compare their results on cellular volume with those obtained with Naftalin's model [9], for different concentrations of apical glucose. It should be noted that we did not simulate ourselves the model from Naftalin.
The data is hard coded in the Python scripts to generate Figure [2]. Those values where then normalized by the cellular volume obtained at the end of the computation with an apical glucose concentration of 0.01 mol/L (10 mM).
Note that without normalization, differences between the values obtained by Afshar et al. and those from Naftalin as seen in Figure 7-bis in this paper appear with about two orders of magnitude.
The two models also predict different responses to increasing luminal glucose concentrations. Afshar et al. predict a reduction in cell volume, whereas Naftalin predicts an increase. This discrepancy was already discussed by Afshar et al. in their article. While we cannot comment on Naftalin's results, our experimental data indicate a decrease in enterocyte cell volume of up to 10% when cells are exposed to 100 mM apical glucose compared with conditions without apical glucose. However, further investigations and independent replication are required before drawing definitive conclusions.

5 Conclusion and Perspectives

In [2], Afshar et al. produced a detailed model of the enterocyte that includes the volume, the membrane potentials, 4 different ionic species and 13 different transporters. We managed to reproduce and reimplement this model from scratch in Julia, and curated the superfluous equations and parameters.
Doing so, it revealed some mistakes in the description of the model, and unexplained behaviors, such as undocumented changing parameters.
Figure 4 in the original paper presents the most ambiguity, as the experimental data from the original paper of Collin et al. [15] does not correspond to the data presented in the figure.
In the future, we will try to match both this model and a simplified one with actual biological data of glucose absorption by the enterocyte and the intestine. A reaction network-based model would also improve both the readability and the reusability of the model.

Data availability

The reproduction is freely available with the following link (https://gitlab.univ-lille.fr/cedric.lhoussaine/glucoseuptake_sglt1_glut2) under the CeCILL-C free softaware licence.

Author contributions

KR redesigned the model, rewrote it in Julia, debugged it and wrote most of the article. CL, CV and MF supervised the thesis, proofread the article and granted advice for the implementation. OB supervised the thesis and proofread the article.

Funding

This work was supported by project MIGAD (ANR-21-CE45-0017) of the French National Research Agency (ANR).

Acknowledgments

The authors would like to thank Dr. V. Suresh for the discussion and Dr. Naftalin for his insight on the enterocyte and the current knowledge on the paracellular pathway.

References

1. N. Afshar, S. Safaei, D. P. Nickerson, P. J. Hunter, and V. Suresh. "Computational Modelling of Glucose Uptake by SGLT1 and Apical GLUT2 in the Enterocyte." In: **Frontiers in Physiology** 12 (Dec. 7, 2021), p. 699152. DOI: 10.3389/fphys.2021.699152. URL: https://www.ncbi.nlm.nih.gov/pmc/articles/PMC8688934/.
2. N. Afshar, S. Safaei, D. Nickerson, P. J. Hunter, and V. Suresh. "Reproducibility Study of Computational Modelling of Glucose Uptake by SGLT1 and GLUT2 in the Enterocyte." In: **Physiome** (Jan. 19, 2023). Publisher: Physiome Incorporated. DOI: 10.36903/physiome.21708179. URL: https://physiome.figshare.com/articles/journal_contribution/Reproducibility_Study_of_Computational_Modelling_of_Glucose_Uptake_by_SGLT1_and_GLUT2_in_the_Enterocyte/21708179.
3. URL: https://gitlab.univ-lille.fr/cedric.lhoussaine/glucoseuptake_sglt1_glut2.
4. L. V. Gromova, S. O. Fetissov, and A. A. Gruzdkov. "Mechanisms of Glucose Absorption in the Small Intestine in Health and Metabolic Diseases and Their Role in Appetite Regulation." In: **Nutrients** 13.7 (July 20, 2021), p. 2474. DOI: 10.3390/nu13072474. URL: https://www.mdpi.com/2072-6643/13/7/2474.
5. G. L. Kellett, E. Brot-Laroche, O. J. Mace, and A. Leturque. "Sugar Absorption in the Intestine: The Role of GLUT2." In: **Annual Review of Nutrition** 28.1 (Aug. 1, 2008), pp. 35–54. DOI: 10.1146/annurev.nutr.28.061807.155518. URL: https://www.annualreviews.org/doi/10.1146/annurev.nutr.28.061807.155518.
6. G. L. Kellett and E. Brot-Laroche. "Apical GLUT2 : A Major Pathway of Intestinal Sugar Absorption." In: **Diabetes** 54.10 (Oct. 2005), pp. 3056–3062. DOI: 10.2337/diabetes.54.10.3056. URL: https://diabetesjournals.org/diabetes/article-pdf/54/10/3056/377839/zdb01005003056.pdf.
7. J. L. Madara and J. R. Pappenheimer. "Structural basis for physiological regulation of paracellular pathways in intestinal epithelia." In: **The Journal of Membrane Biology** 100.1 (Dec. 1987), pp. 149–164. DOI: 10.1007/BF02209147. URL: http://link.springer.com/10.1007/BF02209147.
8. K. Thorsen, T. Drengstig, and P. Ruoff. "Transepithelial glucose transport and Na^+/K^+ homeostasis in enterocytes: an integrative model." In: **American Journal of Physiology-Cell Physiology** 307.4 (Aug. 15, 2014), pp. C320–C337. DOI: 10.1152/ajpcell.00068.2013. URL: https://www.physiology.org/doi/10.1152/ajpcell.00068.2013.
9. R. J. Naftalin. "Does apical membrane GLUT2 have a role in intestinal glucose uptake?" In: **F1000Research** 3 (Dec. 12, 2014), p. 304. DOI: 10.12688/f1000research.5934.1. URL: https://f1000research.com/articles/3-304/v1.

10. N. Afshar, S. Safaei, D. P. Nickerson, P. J. Hunter, and V. Suresh. "Computational Modeling of Glucose Uptake in the Enterocyte." In: **Frontiers in Physiology** 10 (Apr. 12, 2019), p. 380. DOI: 10.3389/fphys.2019.00380. URL: https://www.frontiersin.org/article/10.3389/fphys.2019.00380/full.
11. A. A. Cuellar, C. M. Lloyd, P. F. Nielsen, D. P. Bullivant, D. P. Nickerson, and P. J. Hunter. "An Overview of CellML 1.1, a Biological Model Description Language." In: **SIMULATION** 79.12 (Dec. 2003). Publisher: SAGE Publications, pp. 740–747. DOI: 10.1177/0037549703040939. URL: https://journals.sagepub.com/doi/10.1177/0037549703040939.
12. A. Garny and P. J. Hunter. "OpenCOR: a modular and interoperable approach to computational biology." In: **Frontiers in Physiology** 6 (Feb. 6, 2015). Publisher: Frontiers Media SA. DOI: 10.3389/fphys.2015.00026. URL: http://journal.frontiersin.org/Article/10.3389/fphys.2015.00026/abstract.
13. N. Afshar, S. Safaei, D. Nickerson, P. J. Hunter, and V. Suresh. "Computational Modelling of Glucose Uptake in the Enterocyte." In: **Physiome** (Oct. 1, 2020). Publisher: Physiome Incorporated. DOI: 10.36903/physiome.13034423. URL: https://physiome.figshare.com/articles/journal_contribution/Computational_Modelling_of_Glucose_Uptake_in_the_Enterocyte/13034423.
14. Y. Ma, S. Gowda, R. Anantharaman, C. Laughman, V. Shah, and C. Rackauckas. **ModelingToolkit: A Composable Graph Transformation System For Equation-Based Modeling**. 2021. arXiv:2103.05244 [cs.MS].
15. J. Collin, K. A. Kelly, and S. F. Phillips. "Increased canine jejunal absorption of water, glucose, and sodium with intestinal pacing." In: **The American Journal of Digestive Diseases** 23.12 (Dec. 1978). Publisher: Springer Science and Business Media LLC, pp. 1121–1124. DOI: 10.1007/bf01072888. URL: http://link.springer.com/10.1007/BF01072888.

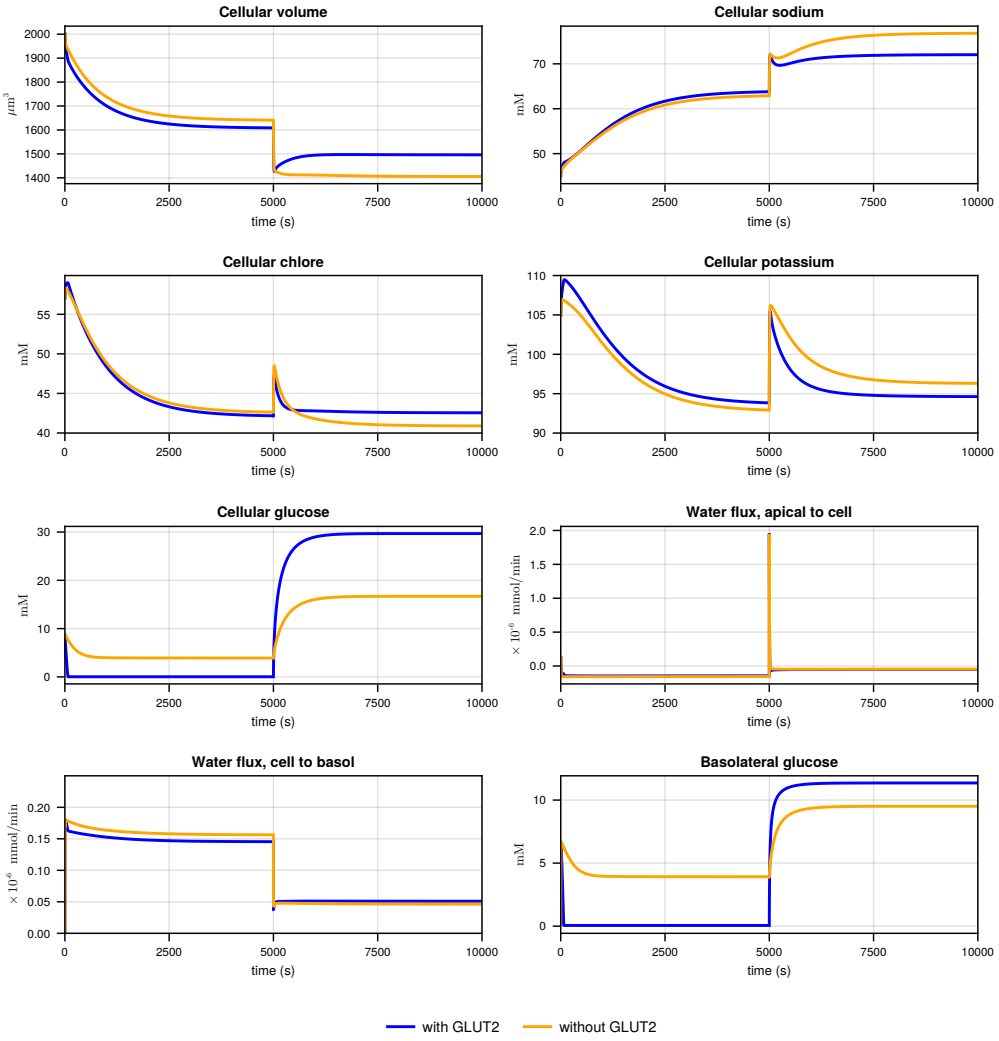

Figure 1. Blue line: with apical GLUT2 (pathways **1**, **2** and **3** in Figure Enterocyte). Orange: without apical GLUT2 (pathways **1** and **3** only in Figure Enterocyte). Variation of the cellular volume, the cellular concentration of sodium, chloride, potassium and glucose, the apical flow of water, the basolateral flux of water and the basolateral concentration of glucose. At $t = 0$ s, the concentration of apical glucose is set to zero until $t = 5000$ s when apical glucose is set to 50 mM.

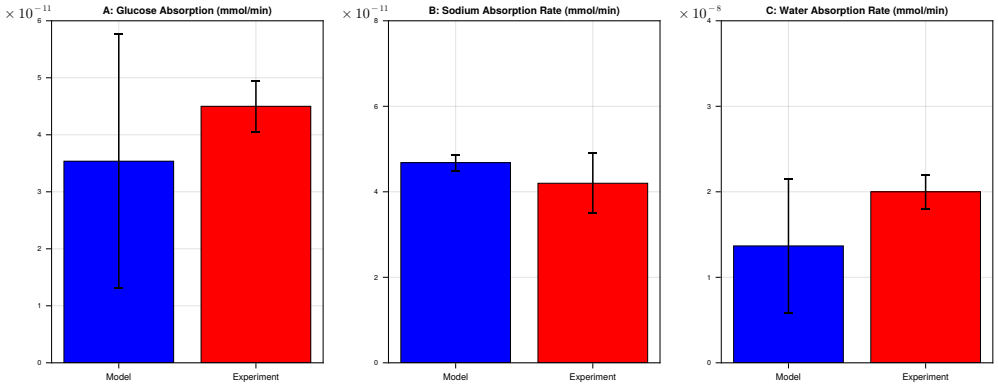

Figure 2. Absorption rates of glucose from the cell to the lumen (**A**), of sodium from the apical side to the cell (**B**), and of water from the apical side to the cell (**C**). The values shown represent the mean and standard deviation obtained from four seperate runs where the parameter `Q_in` was varied [6×10^{-18}, 1×10^{-17}, 3×10^{-17}, 1×10^{-15}]. `Q_in` is the capillary flow. The red bar is supposedly originated from Collins et al. [15]

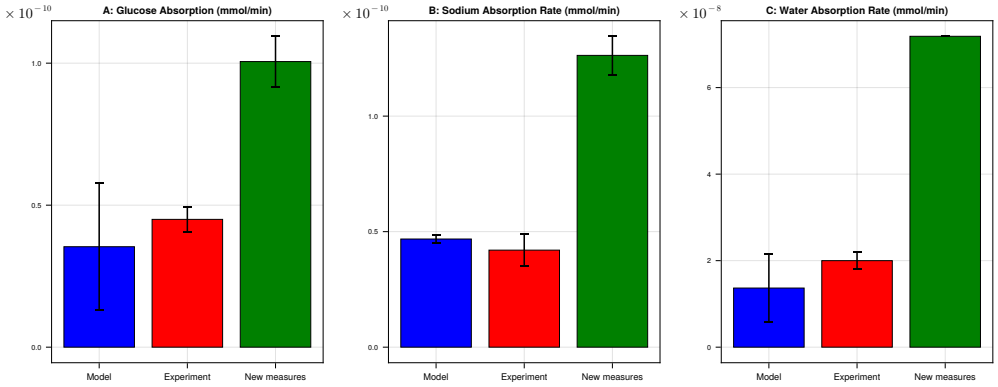

Figure 2-bis. Figure 2 in [2] modified with the values of experimental data from Collins et al. [15] as we measured it.

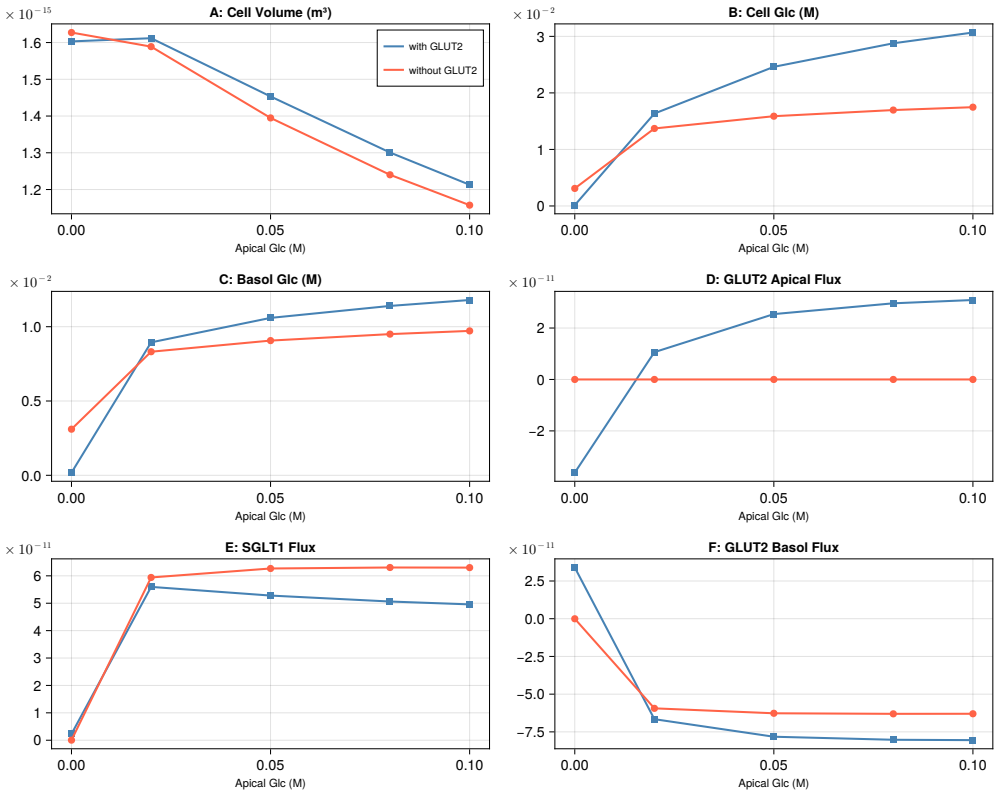

Figure 3. Final value after a run for different values of apical glucose. Comparison with and without the apical GLUT2 transporter. Cellular Volume (**A**), concentration of cellular glucose (B), basolateral glucose (**C**), flux of glucose through the apical GLUT2 transporter (**D**), flux of glucose through SGLT1 (**E**) and flux of glucose through the basolateral GLUT2 (**F**).

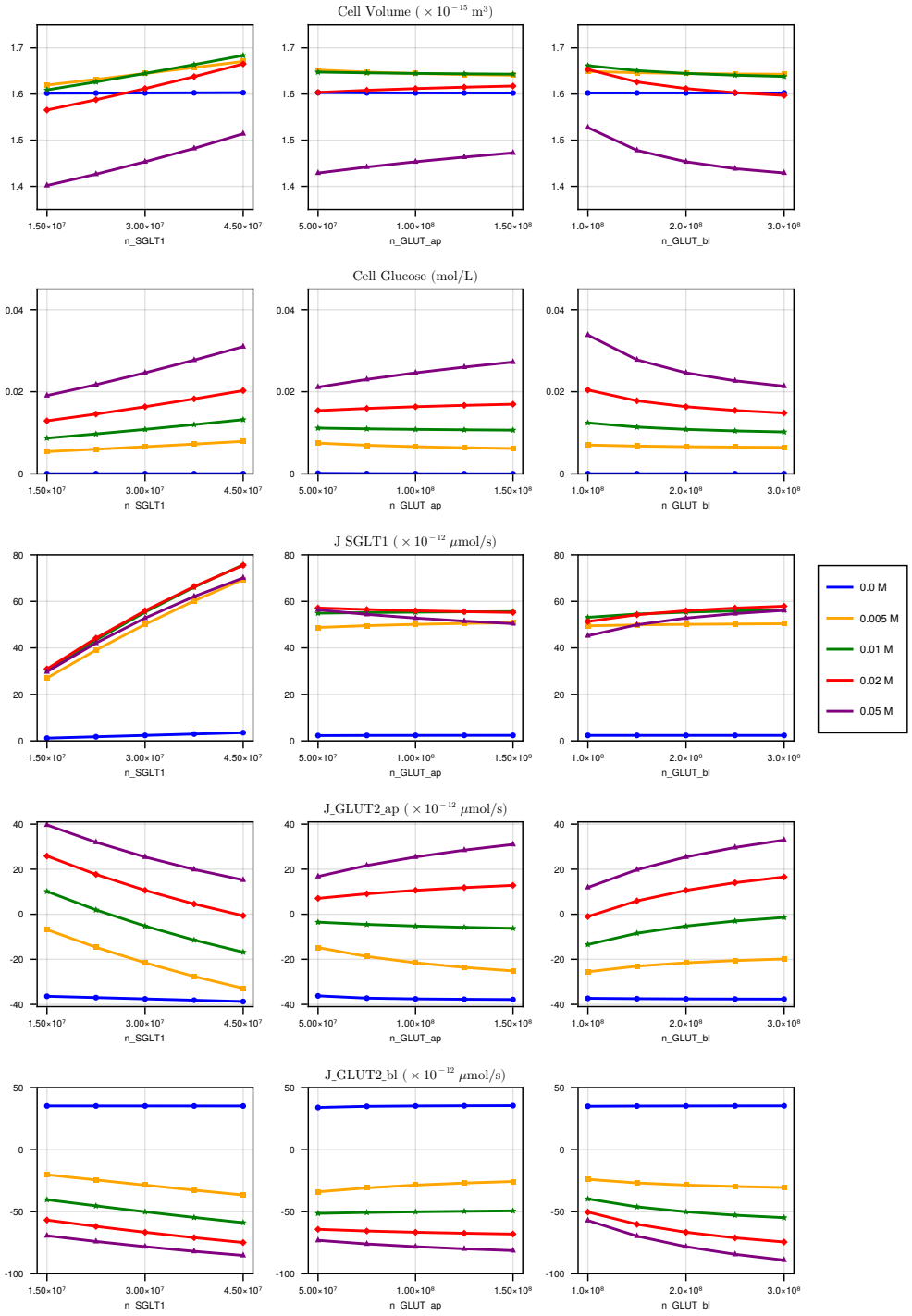

Figure 4. Variation of cellular volume (first row), concentration of cellular glucose (second row), flux of glucose through SGLT1 (third row), through apical GLUT2 (fourth row) or through basolateral GLUT2 (fifth row). Three different conditions are studied: with different quantities of SGLT1 (first column), of apical GLUT2 transporter (second column) or basolateral GLUT2 transporter (third column). Different conditions of apical glucose are studied (blue: 0mM, yellow: 5mM, green: 10mM, red: 20mM, purple: 50mM).

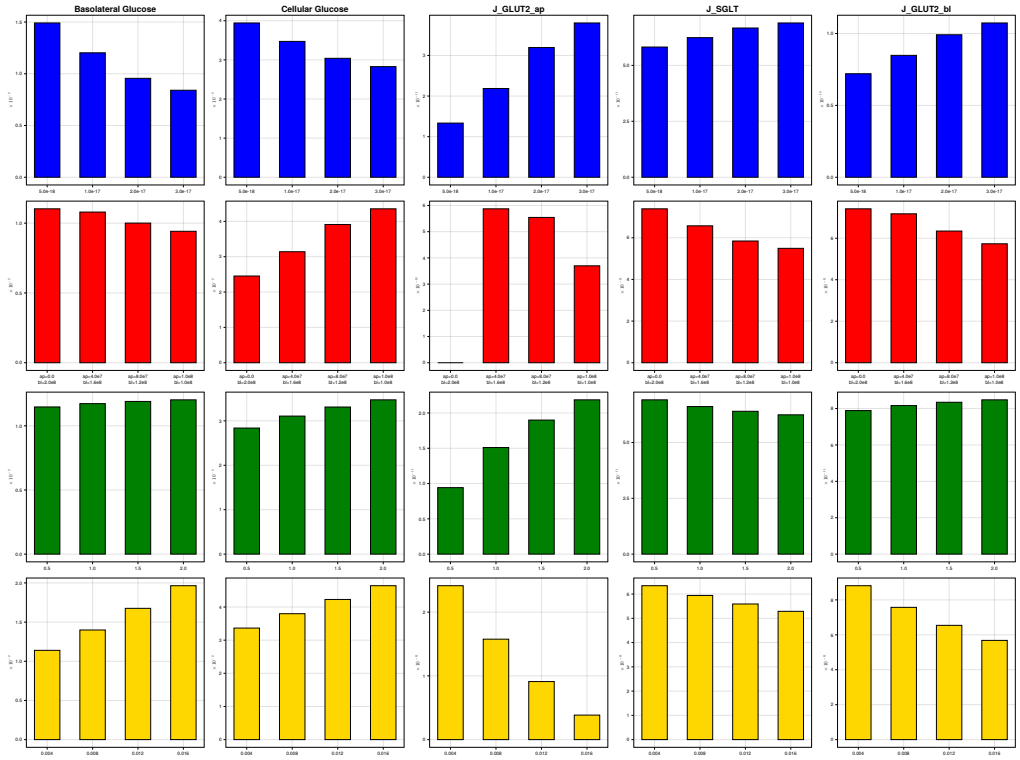

Figure 5. Final value of the concentration of basolateral glucose (first column), cellular glucose (second column), and fluxes of glucose through apical GLUT2 transporters (third column), SGLT1 (fourth column) and basolateral GLUT2 (fifth column). The simulations were run with different parameters, with variations of that parameters around a default value. First row studies the variation of `Q_in`, the flow of capillaries. Second row studies what would happen if the basolateral GLUT2 transporter was moved from basolateral to apical membrane (removal of basolateral GLUT2 with addition of the same quantity to apical GLUT2). Third row shows if apical GLUT2 was added without withdrawal of basolateral GLUT2. Fourth row studies the influence of an input of glucose by the blood to the basolateral membrane (intake by capillaries), which might represent what could happen in case of a higher blood sugar levels (as in diabetes).

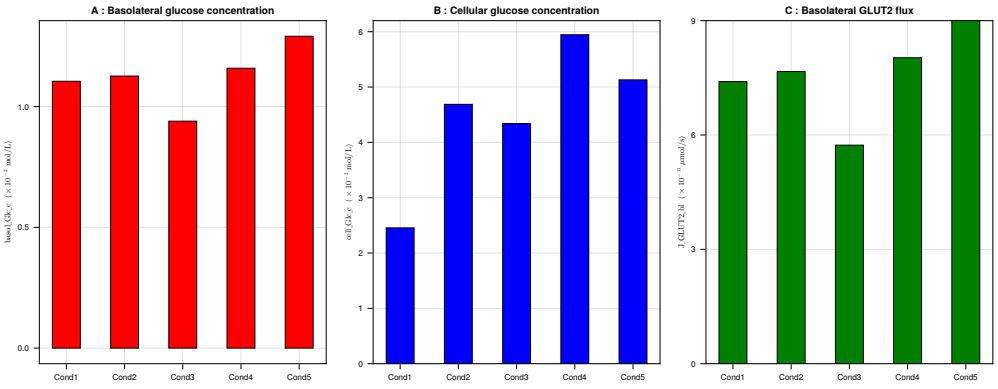

Figure 6. Variation of the final time of simulation for different quantities of SGLT1, apical and basolateral GLUT2 as shown in Table 2. The variables studied are the concentration of basolateral glucose (**A**), cellular glucose (**B**) and flux of glucose through basolateral GLUT2 (**C**).

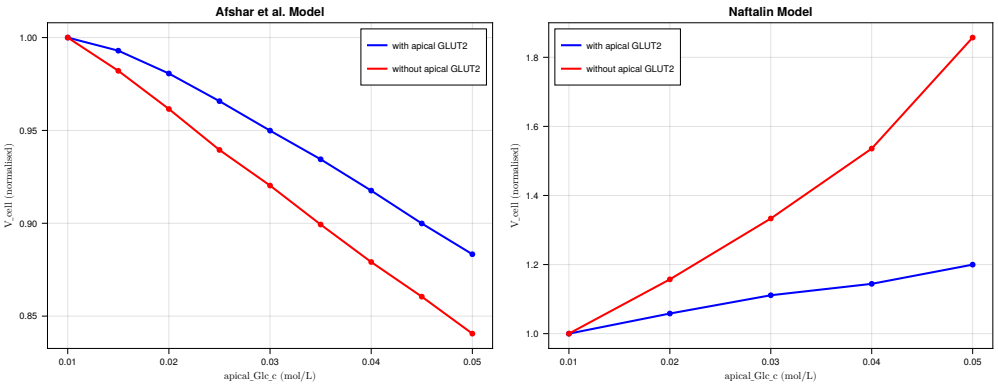

Figure 7. Final value of cellular volume for different apical glucose concentrations. Right panel reports the values of Naftalin's simulations [9]. The values are normalized by the first value at 10mM of apical glucose in each model.

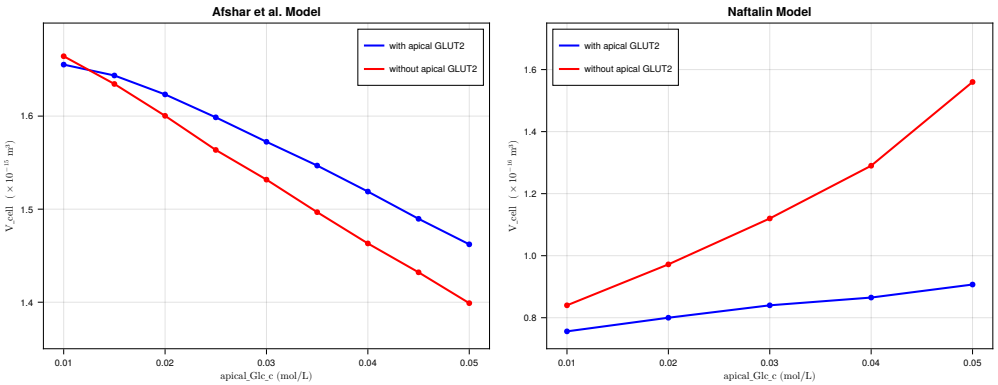

Figure 7-bis. Same as Figure 7, but without normalization.